ELSEVIER

Marine Geology 207 (2004) 169–184

MARINE GEOLOGY
INTERNATIONAL JOURNAL OF MARINE GEOLOGY, GEOCHEMISTRY AND GEOPHYSICS

www.elsevier.com/locate/margeo

Spatial and temporal variations in wave characteristics across a reef platform, Warraber Island, Torres Strait, Australia

Robert W. Brander[a,*], Paul S. Kench[b], Deirdre Hart[c]

[a] *School of Biological, Earth and Environmental Sciences, University of New South Wales, Sydney 2052, Australia*
[b] *School of Geography and Environmental Science, University of Auckland, Private Bag 92019, Auckland, New Zealand*
[c] *School of Physical, Environmental and Mathematical Sciences, UNSW ADFA, Canberra 2600, Australia*

Received 23 July 2003; received in revised form 11 February 2004; accepted 23 March 2004

Abstract

A field experiment was conducted at Warraber Island, Torres Strait, Australia to investigate spatial and temporal variations in wave characteristics and energy across a mesotidal coral reef platform. Measurements of water depth were obtained using five pressure sensors deployed across a 2.7-km section of reef flat from July 3–5, 2001. The reef surface was uneven and consisted of an outer reef flat, a central reef flat depression, an inner reef ramp, a palaeo-reef surface and the shoreline. Water levels decreased landward across the platform with tide ranges at the shoreline being almost 50% lower than at the outer reef flat. Rising and falling tides were characterised by a bimodal energy distribution with both short-period (0–3 s) and wind (3–8 s) waves present. Higher water levels were dominated by wind waves. The highest waves occurred at high tides associated with nocturnal tidal cycles with H_s decreasing from 0.5 to 0.2 m from the outer reef flat to the shoreline. Wave energy at swell (8–20 s) and infragravity (>20 s) frequencies was negligible across the reef platform although there was evidence of wave groups at higher water levels.

Reef geometry and changes in water level determine the magnitude of wave energy on the reef platform. Up to 85–95% of incident wave energy is attenuated by the central reef flat depression at high and low tide, respectively, and strong linear relationships exist between H_s and h at all locations. Both wave height and wave type are strongly depth dependent. Critical reef rim depths required to produce H_s of a given size vary spatially across the reef rim due to variations in reef topography. A distinct depth related threshold exists at which short-period and wind wave dominance reverses. Over a 14-day spring-neap tidal cycle, the time of occurrence of wave action diminishes across the reef platform to the shoreline. Larger waves ($H_s = 0.2$ m) occur for only 9% of time at the outer reef flat and for less than 0.5% over the remaining reef platform. This implies that on mesotidal reef platforms, sediment entrainment and transport are severely constrained under normal wave energy conditions and significant change is likely restricted to extreme events.

Keywords: coral reefs; hydrodynamics; wave transformation; reef platform; Torres Strait

1. Introduction

Coral reef islands are low-lying subaerial accumulations of unconsolidated sediments deposited on reef platforms. Considerable variation exists in the size and

* Corresponding author. Fax: +61-2-9385-1558.
E-mail addresses: rbrander@unsw.edu.au (R.W. Brander), p.kench@auckland.ac.nz (P.S. Kench), dehart@ihug.co.nz (D. Hart).

0025-3227/$ - see front matter © 2004 Elsevier B.V. All rights reserved.
doi:10.1016/j.margeo.2004.03.014

elevation of islands, and the textural characteristics of their sediments and numerous classification schemes have been developed to account for these differences (e.g., Spender, 1930; Steers, 1937; Fairbridge, 1950; Stoddart and Steers, 1977). In general, islands formed in low-energy reef settings are comprised predominantly of sand-size sediments and are referred to as sand cays. The sediment which comprises these islands is bioclastic in origin and is generated solely from the adjacent reef system (e.g., McLean and Stoddart, 1978; Hopley, 1982). Consequently, island growth, maintenance and change are reliant on the transport of sediments from the reef source to the island sink (Gourlay, 1988). As noted by Hopley (1982), the most important factor controlling these sediment transfers is the complex interaction of waves and currents operating on the reef surface.

Sand cays are morphologically more unstable than their sand and gravel counterparts, termed motu (Stoddart and Steers, 1977), and can change size, shape and elevation in response to changes in incident energy conditions (e.g., Flood, 1974; Hopley, 1981). While it is recognised that gross reef-top processes control sediment dispersal, little is known regarding the specific hydrodynamic controls on sediment entrainment, transport and deposition across reef surfaces that ultimately contribute to the development and stability of island shorelines. In particular, the role of waves and the range of wave types across the reef platform that control island morphodynamics are poorly understood.

Hydrodynamic studies in coral reefs can be divided into two groups: those focussing on broad scale circulation and flushing of reef and lagoon systems (e.g., Frith, 1982; Frith and Mason, 1986; Hearn and Parker, 1988; Wolanski and King, 1990; Prager, 1991; Kench, 1994; Kraines et al., 1998; Yamano et al., 1998) and those examining the interaction and transformations of incident swell energy against reef platforms. This latter group can be further differentiated into studies that have focussed on wave set-up and set-up driven currents at the reef edge (e.g., Tait, 1972; Gerritsen, 1981; Seelig, 1983; Gourlay, 1990; 1996a,b; Symonds, 1994; Symonds et al., 1995; Tartinville and Rancher, 2000); studies of wave energy dissipation and transformation (e.g., Roberts et al., 1977; Roberts and Suhayda, 1983; Young, 1989; Lee and Black, 1987; Hardy and Young, 1991; Hardy et al., 1991; Massel, 1992; Roberts et al., 1992; Gourlay, 1994; Kench, 1998; Lugo-Fernandez et al., 1998a,b; Hearn, 1999; Tsukayama and Nakaza, 2001), and hydraulic roughness and mass transport (e.g., Nelson, 1996; Hearn et al., 2001; Baird et al., in press).

To date, research has focused on a two-dimensional (ocean to lagoon) treatment of reef platforms and the limiting assumption that transformations occur perpendicular to the reef crest across an over-simplified reef structure with near-horizontal surfaces and an absence of significant topographic features. The existence of rubble ridges, palaeo-reef surfaces, lagoons and islands will likely exert an influence on the characteristics and transformation of waves across reef platforms that ultimately interact with island shorelines. Furthermore, it should be emphasised that most studies have focussed on a relatively narrow region encompassing the forereef, reef crest and immediate backreef lagoon. Consequently, there is a paucity of hydrodynamic data across reef platforms to island shorelines on which to evaluate the role of waves and currents on reef sediment transport and island development. This study presents data from a detailed investigation of wave processes across a 2.7 km reef platform on Warraber Island, a coral sand cay situated in Torres Strait, Australia. The aims of the study are to: (i) describe spatial and temporal variations in wave characteristics and energy across the reef platform; and (ii) quantify the period of time that segments of the reef system are influenced by different types of wave activity over both individual and neap-spring tidal cycles. Results are used to identify those components of the wave field most critical to island development and change.

2. Field site

2.1. Geology

Torres Strait is a shallow (15–25 m deep) shelf situated between the northernmost point of the Cape York Peninsula, Australia and Papua New Guinea (Fig. 1). The Strait acts as the only conduit for water flow between the Coral Sea (from the east) and Gulf of Carpentaria (to the west). The Warraber reef platform (10°13′ S, 142°50′ E) is located in the southern

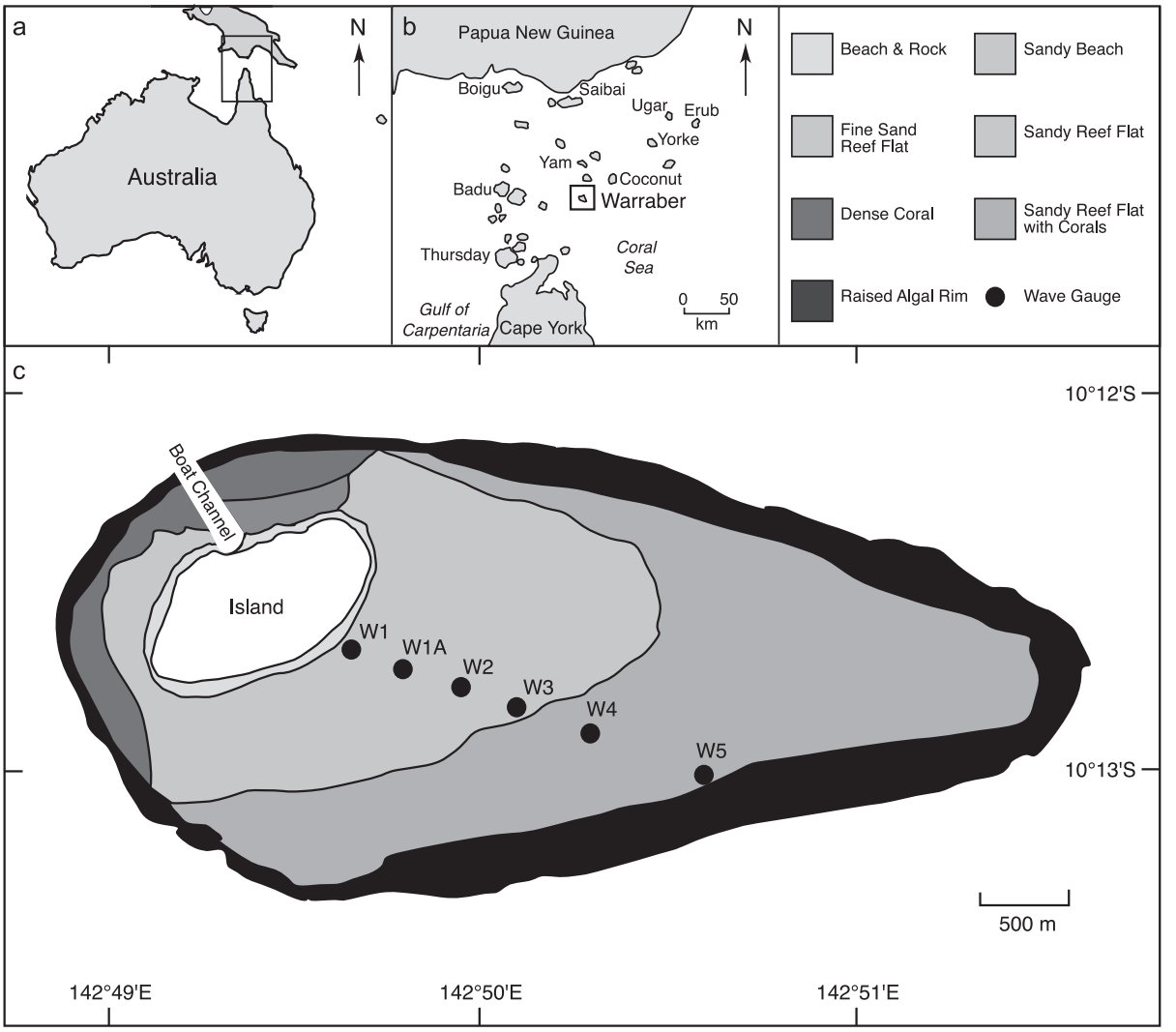

Fig. 1. Location of study site indicating: (a) Torres Strait; (b) Warraber Island; and (c) the island and reef platform system including ecologic zones and instrument locations (W1, W1A, . . ., W5).

portion of the Warrior Reefs physiographic region of the Strait (Jennings, 1972; Hopley, 1982). This region comprises platform reefs which have developed on top of a shallow (15–18 m) basement ridge and are divided by channels scoured by tidal currents to depths as great as 27 m (Hopley, 1982). Warraber reef is an elongated reef platform oriented east to west with a long axis of 5 km and a maximum width (north to south) of 2.5 km (Fig. 1). The surface geology of the reef platform is Holocene in age, and Woodroffe et al. (2000) suggest that it reached a level above present sea level 5000–5500 years BP. Warraber Island is located on the western edge of the reef platform (Fig. 1c). Based on radiocarbon dates, Woodroffe et al. (2000) also suggest that the island is 4500 years in age.

2.2. Hydrodynamic setting

The prevailing winds in Torres Strait are south-easterly, although the northwest monsoon creates calm wind conditions from December to March

(Hopley, 1982). During the experiment, winds were steady (6.2 m s^{-1}) from the southeast (115°). Mean monthly global wave climate data for the Warraber region (Young, 1999) indicate that significant wave heights (H_s) range from 1.9 to 2.7 m from October to April. Between May and September, H_s ranges from 1.4 to 1.8 m. Spectral peak wave periods (T_p) vary from 8 to 10 s with minimum values associated with low H_s (May–September). Waves are from the NE during the extended summer period and E to SE during winter. In July, when the experiment was conducted, waves are generally ESE (109°) with H_s and T_p of 1.4 m and 8.4 s, respectively (Young, 1999). Torres Strait is mesotidal with a mean spring tidal range of 3.6 m. The combination of narrow channels between islands and the dissimilar and out of phase tidal systems between the Coral Sea and Gulf of Carpentaria create strong currents exceeding 2.5–4 m s^{-1} in places (Amin, 1978; Harris, 1988; Bode and Mason, 1994). These tidal currents have likely exerted a strong control on the structure and morphology of reefs within the Strait with many being elongate in a west–south orientation.

2.3. Reef topography and zonation

This study reports on hydrodynamic measurements undertaken across a reef transect extending 2700 m southeast of the island shoreline (Fig. 1) and the topography of the reef platform surface is shown in Fig. 2. The reef platform can be divided into six distinct zones based on geomorphic and ecological characteristics (Figs. 1 and 2).

The *outer reef rim* consists of a pronounced reef crest with a living veneer of encrusted red algae, with sparse coral colonies and algal turf. There is little loose sediment deposited in this zone. The reef crest is up to 0.5 m higher in elevation than the central reef (Fig. 2). Immediately landward of the reef rim, the outer reef flat surface dips landward (0.04°) for 625 m toward a central depression (Fig. 2). This zone consists of outcrops of dense coral cover (approximately 20%) and 15% algae with a veneer of coarse sand. The *central reef flat depression* represents a nearly horizontal 1000 m wide zone which is 0.3–0.5 m lower in elevation than the reef rim (Fig. 2). It is dominated by sand and gravel-sized sediment (40–47% cover) with an outer

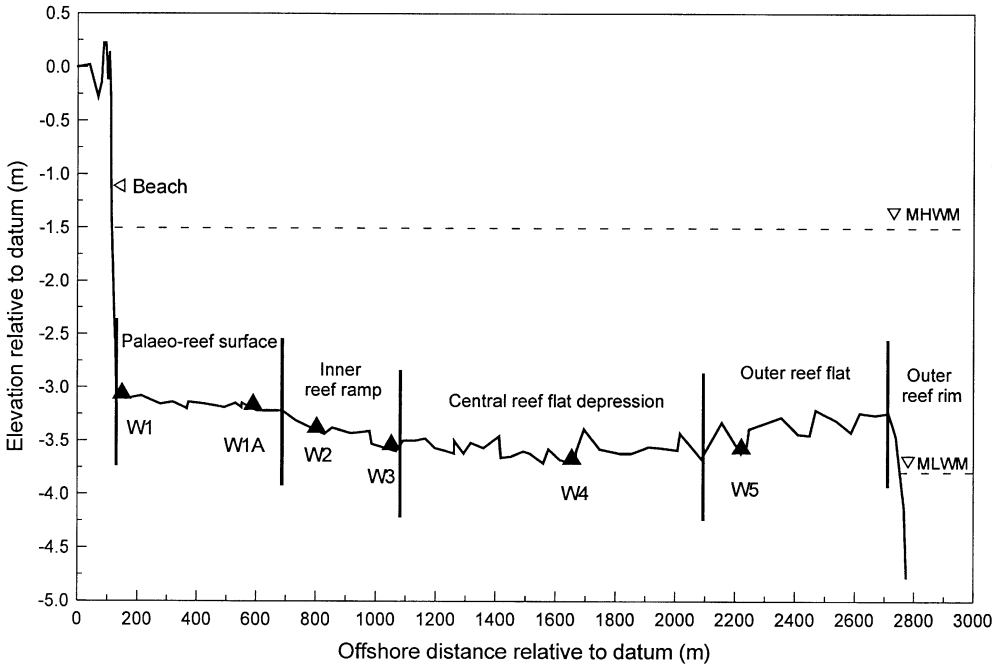

Fig. 2. Reef transect profile on the southeast (120°) side of Warraber Island. Instrument locations are shown (W1, W1A . . . W5) and topographic regions are separated by vertical bars.

zone of isolated dense coral outcrops (25% cover), coralline algae (20%), minor addition of Halimeda and fleshy algae (15%) and an inner zone with only isolated coral colonies (8% cover), coralline algae (30% cover), 5% Halimeda and 10% fleshy algae.

At the landward extent of the central depression, the reef surface increases in elevation across a 430-m ramp. This seaward dipping (0.04°) *inner reef ramp* is devoid of living coral and is dominated by sand-sized sediments with approximately 25% cover of coralline algae and 23% fleshy algae. This ramp terminates at an *inner palaeo-reef surface* that dips gently seaward (0.02°) and at its highest point (toe of beach) is 0.17 m higher in elevation than the elevated reef rim (Fig. 2). The palaeo-reef is approximately 500 m in width at the surveyed location and is devoid of living coral and coralline algae. This zone is exposed for much of the tidal cycle and is covered with sand-sized sediment in which gastropods are a dominant constituent. The sand cover is approximately 5–15 cm thick and overlies coral rubble and rock. Isolated dead and eroded coral colonies protrude through the sand matrix. Radiocarbon dates on individual microatolls yielded dates of 5210–5320 years BP indicating this part of the reef formed at a time of higher sea level in the late Holocene (approximately 5000 years ago; Woodroffe et al., 2000). The lower elevation outer reef platform zones are considered to represent reef flat development subsequent to sea level fall to present day level approximately 3000 years ago (Woodroffe et al., 2000). The palaeo-reef surface adjoins the toe of beach at a marked break in slope often dictated by water table outcropping. The *beach* is steep (8°) and featureless, having a width of 18 m and is comprised of medium to coarse sands dominated by gastropods.

3. Methods

Hydrodynamic instruments were deployed across a central reef transect located on the southeast (120°) side of the island (Fig. 1c). Surveying was performed using a standard auto level, with all surveys reduced to a common temporary benchmark located landward of the island foredune. Measurements of water surface elevation were obtained using a range of instruments: a Druck 1830 pressure transducer hard-wired to a shore based data acquisition system, two standalone Inter-Ocean S4 wave and current meters (256 Kb and 20 Mb memory), and standalone Dobie and Seabird wave gauges. These instruments were mounted on weighted pods fixed to the reef surface and were deployed at five locations (denoted as W1, W1A, W2, W3, W4 and W5) across the reef platform encompassing each of the topographic reef zones except for the outer reef slope (Figs. 1c and 2). Additional tide level information was obtained from water level predictions for nearby Poll Island.

Measurements were obtained between July 3 and 5, 2001 during a period of spring tides and encompassed three consecutive high tides (Fig. 3a): a higher noctur-

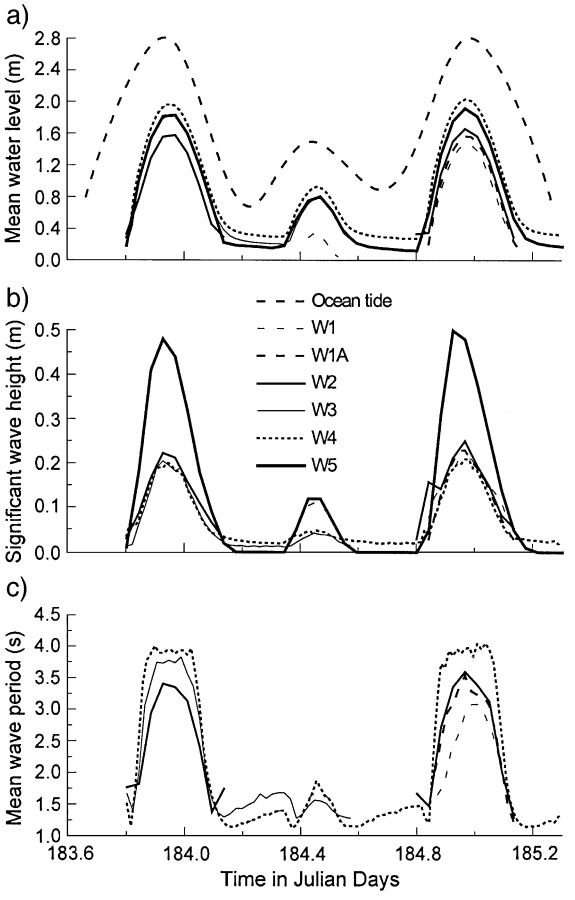

Fig. 3. Temporal variations of: (a) mean water depth, h; (b) significant wave height, H_s; and (c) mean significant wave period, T_s; recorded at the instrument stations between 1915 h on July 3 (Julian Day = 183) and 1100 h on July 5 (Julian Day = 185). W1, W1A ... W5 refer to instrument locations.

nal high tide (HHT1) on 3–4/7/01, a lower daytime high tide (DHT) on 4/7/01 and another higher nocturnal high tide (HHT2) on 4–5/7/01. Due to the diurnal tidal inequality, measurements were concentrated around the higher nocturnal tides. After the first two tidal cycle measurements from July 3 to 4, the Dobie wave gauge was moved from W3 to W1A (Fig. 1c).

Sampling frequency and duration varied due to instrument constraints and the different times of exposure of the reef platform. All instruments sampled at a rate of 2 Hz with the exception of the shore based Druck pressure sensor (W1), which sampled at 4 Hz. Sampling intervals and durations varied and are summarized in Table 1. Estimates of significant wave height (H_s) were obtained using the standard deviation (σ) of the pressure sensor records; $H_s = 4\sigma$ (Aagaard and Masselink, 1999). Significant wave period (T_s) was determined through zero-downcrossing analysis. Auto-spectral analysis was used to determine peak wave period (T_p) and the amount of variance associated with incident short-period wave frequencies of 0–0.333 Hz (0–3 s), incident wind wave frequencies of 0.333–0.125 Hz (3–8 s), incident swell wave frequencies of 0.125–0.05 Hz (8–20 s), infragravity wave frequencies of 0.05–0.01 Hz (20–100 s) and far-infragravity wave frequencies of <0.01 Hz (>100 s). The proportion (%) of energy within each frequency band in a given time series record was computed by dividing the variance in that band by the total variance in the time series.

4. Reef flat water levels

There was a general trend of decreasing water depth across the Warraber reef platform from the reef rim landward to the toe of beach (Fig. 3a) and maximum water depths at W4 indicate the variation of reef elevation (Fig. 2). Water level records also show a number of key changes in range and asymmetry when compared with the ocean tide (Fig. 3a). The ocean tide range for the three tidal cycles was 2 m (HHT1), 0.8 m (DHT) and 1.9 m (HHT2). In comparison, the sensor closest to the reef rim (W5) recorded tide ranges of 1.64, 0.65 and 1.80 m indicating a reduction in tide range of 0.36, 0.15 and 0.1 m, respectively. While measured tidal ranges are similar between the outer two sensors (W5 and W4), there is a marked reduction in tidal range on the central to inner reef flat (Fig. 3a). The smallest measured tidal range is found at the toe of beach (W1), being 0.35 m for DHT and 1.47 m for HHT2. These values represent 46% and 19% of the tide range measured at site W4. Differences in tidal range reflect differences in reef height with higher elevation sections of the reef platform truncating the tidal signature (Fig. 2). These results clearly show the ocean tide falls below the level of the reef at lower tidal stages and that reef elevation exerts a major control on effective tide range across the reef platform.

Tidal curves on the reef flat were asymmetric at all locations with rapid flood and ebb phases and extended periods of gradual water level fall toward low tide. Locations that are permanently inundated exhibit sharp and rapid transitions between low tide and the flood- and ebb-tide phases (Fig. 3a). During early phases of reef flat tidal inundation, water levels increased rapidly at rates of 2–3 cm s^{-1}. These patterns are largely a function of the tide rising and falling below the level of the outer reef rim. At low tide, the reef rim imposes a physical constraint on

Table 1
Summary of instrument sampling design

Location	Sensor	Sampling			
		Rate	Start (h – date)	Stop (h – date)	Duration
W1 (beach toe)	Druck	4 Hz	1015–4/7/01 2022–4/7/01	1307–4/7/01 0250–5/7/01	continuous
W1A (palaeo-reef)	Dobie	2 Hz	1915–4/7/01	1402–5/7/01	17.1 min every 30 min
W2 (inner reef ramp)	S4 256 Kb	2 Hz	1915–3/7/01 1915–4/7/01	0335–4/7/01 0427–5/7/01	20 min every 1 h
W3 (inner reef ramp)	Dobie	2 Hz	1915–3/7/01	1422–4/7/01	17.1 min every 30 min
W4 (central depression)	S4 20 Mb	2 Hz	1915–3/7/01	1000–5/7/01	continuous
W5 (outer reef flat)	Seabird	2 Hz	1015–3/7/01	17/7/01	17.1 min every 1 h

propagation of the tide onto the reef. Water ponded on the reef flat continued to drain off the platform, contributing to the gradual water level fall at low tide (Fig. 3a).

5. Wave height and period

Selected 3-min water elevation records and wave energy spectra (associated with the entire 20-min record) from the central reef flat (W2) are shown in Fig. 4. The time series and spectra are representative of the typical changes in the character of waves (height and period) found at all locations during both nocturnal tidal cycles and indicate the marked transition in the height, period and groupiness of waves propagating across the reef surface at different tidal stages. As water level rises and inundates the reef platform, the wave record is dominated by low amplitude waves and is characterized by a bimodal energy distribution with broad peaks in both the short-period (0–3 s) and wind wave (3–8 s) bands, with the former being slightly dominant. An additional energy peak associated with infragravity frequencies is also present (Fig. 4a). At maximum water depth, water level records are characterized by significantly higher waves ($H_s = 0.1–0.2$ m) dominated by a narrow band of wind wave frequencies (3–5 s). Of note, waves occur in groups of four to six individual waves (Fig. 4b). Energy at infragravity frequencies is greater than during the rising tide, but is insignificant in proportion to the wind wave energy. By early to mid-falling tide, the wave groups are absent from the wave record (Fig. 4c) and the wave characteristics and spectral variance are similar to conditions during the rising tide with peaks at short-period, wind wave and infragravity frequencies. At low water levels, no significant wave action is present in the records and no discernible spectral variance pattern is evident.

Changes in primary wave characteristics at each location over the entire experiment are presented in Fig. 3b. Significant wave height (H_s) is directly related to water depth on the reef platform, reaching maximum and minimum values at high and low tides, respectively, at all locations. The highest values of H_s were just under 0.5 m and were recorded landward of the reef rim (W5). There is a significant reduction in H_s (58%) between W5 and W4, over a distance of 556 m, while values of H_s between W4 and W1 are similar in magnitude. However, there is a subtle shift in H_s, which increased landwards towards a smaller maximum at W2, before decreasing slightly again towards the shoreline (Fig. 3b). Of note, H_s values are much lower at all locations during the DHT, reaching a maximum of 0.12 m near reef edge (W5) and 0.04 m close to the shoreline (W1).

Significant wave period (T_s) is also strongly correlated with water depth on the reef platform. Maximum values of T_s range from 3 to 4 s and occur around high tide. On the central and outer reef locations (W4 to W3), wave period increases rapidly during the rising tide and stabilizes for several hours around high tide. In contrast, the increase in wave period is more peaked in the inner reef flat locations (W2 to W1) indicating that longer period wave energy occurs for a much shorter time in any tide at these locations (Fig. 3c). In general, T_s decreases from the reef edge to island shoreline during all stages of the tide. Minimum values of T_s were associated with mid- to low-tide stages and ranged from 1 to 2 s. During the extended low-tide period, there was a tendency for T_s to increase gradually until the onset of the flooding tide (Fig. 3c), likely due to wind wave forcing across the ponded water surface.

6. Wave energy

In order to further assess the types and amounts of wave energy acting across the reef, wave energy was grouped into the five categories described in Section 2. Fig. 5 clearly illustrates that wave energy across the reef flat is dominated by wind wave frequencies (3–8 s). The development of wind waves is strongly correlated to water depth with energy in this wave band increasing rapidly from mid-rising tide, peaking sharply at high tide, and decreasing rapidly to mid-falling tide stages (Fig. 5c). The dependence on development of wind wave energy on water depth is evident during the DHT where water level was not sufficient for development of energy in this wave band. No distinct spatial relationship is apparent with wind wave energy being highest at W2 and W4 and lowest at W1.

Short-period wave energy (0–3 s) is also important on the reef platform, but is approximately 70–

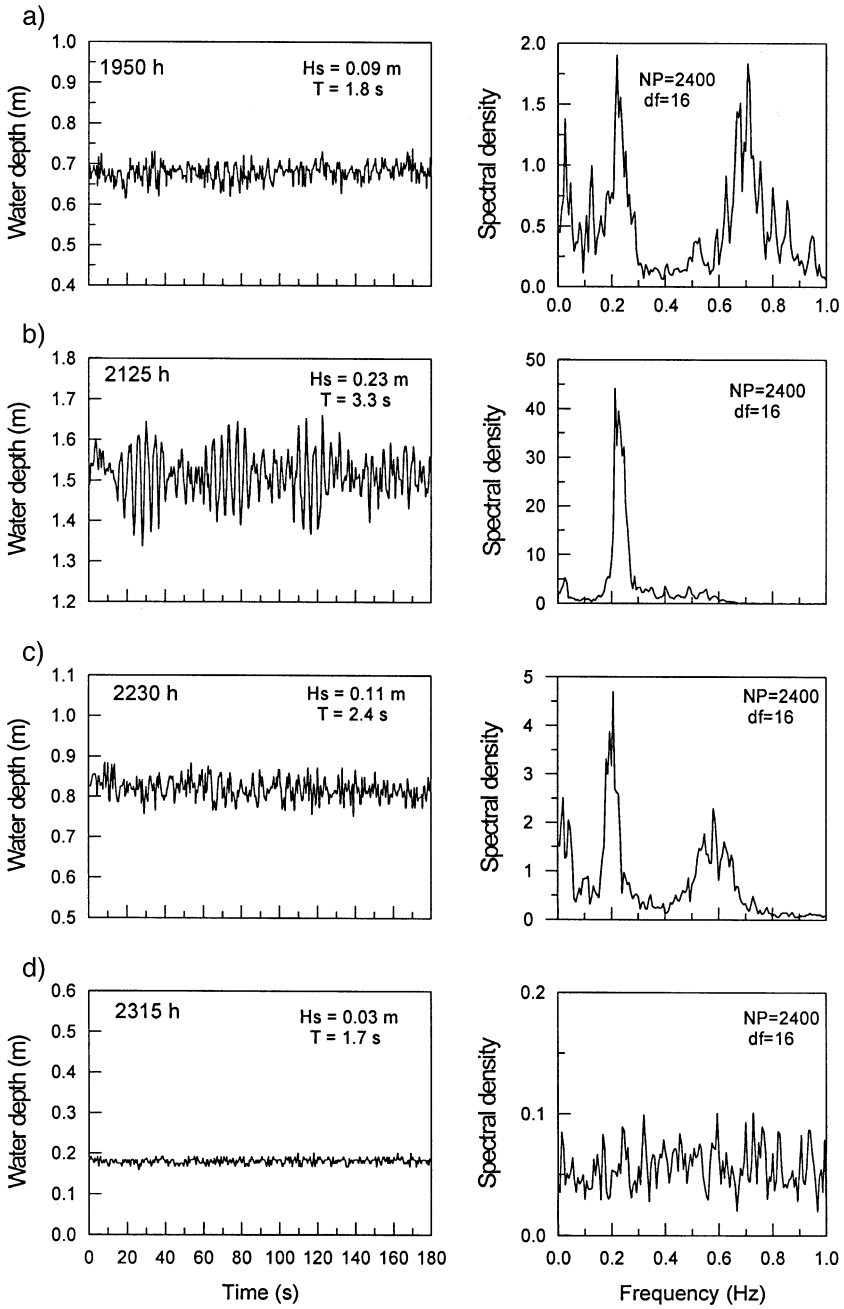

Fig. 4. Examples of 3-min water level records and wave energy spectra (for the associated 20-min burst) on the inner reef ramp (W2) during the nocturnal tide (HHT1) on 3/7/01 for: (a) the flooding tide; (b) high tide; (c) ebbing tide; and (d) low tide. H_s = significant wave height; T = mean wave period; NP = number of points in record; df = degrees of freedom. Spectral density is in units of $m^2\ Hz^{-1} \times 10^{-3}$.

80% lower in magnitude than the wind wave frequency (Fig. 5b). Development of short-period wave energy is also tidally modulated, but in contrast to wind wave energy, is prevalent at lower tidal stages and exhibits a longer and broader peak around high tide. Short-period wave energy reaches a maximum

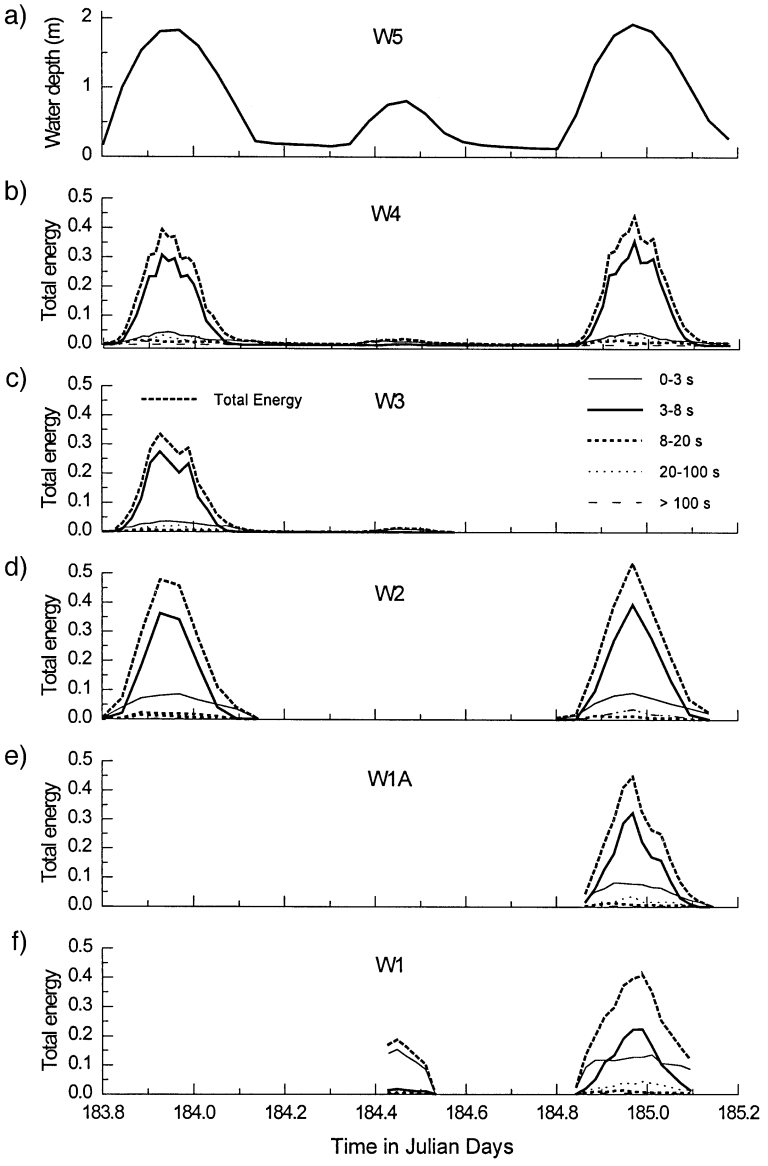

Fig. 5. Temporal variation in wave energy across the reef platform showing: (a) water depth at W5; (b) short-period waves (0 – 3 s); (c) wind waves (3 – 8 s); (d) swell waves (8 – 20 s); (e) infragravity waves (20 – 100 s); and (f) far-infragravity waves (>100 s). Energy is in units of m^2 Hz^{-1}). W1, W1A . . . W5 refer to instrument locations.

at the shoreline (W1) for both the DHT and HHT2, and was the dominant wave frequency during the DHT. In general, the magnitude of short-period wave energy tended to increase onshore across the reef platform. Energy at swell (Fig. 5d) and far-infragravity (Fig. 5f) wave frequencies were negligible, but there is evidence of increasing infragravity energy (Fig. 5e) towards high tide at all locations across the reef.

Examination of the percentage of total wave energy made up by the five wave frequency bands clearly indicates that at all locations on the reef platform, wind waves dominated at high tide and short-period waves dominated at low tide (Fig. 6). The transition between

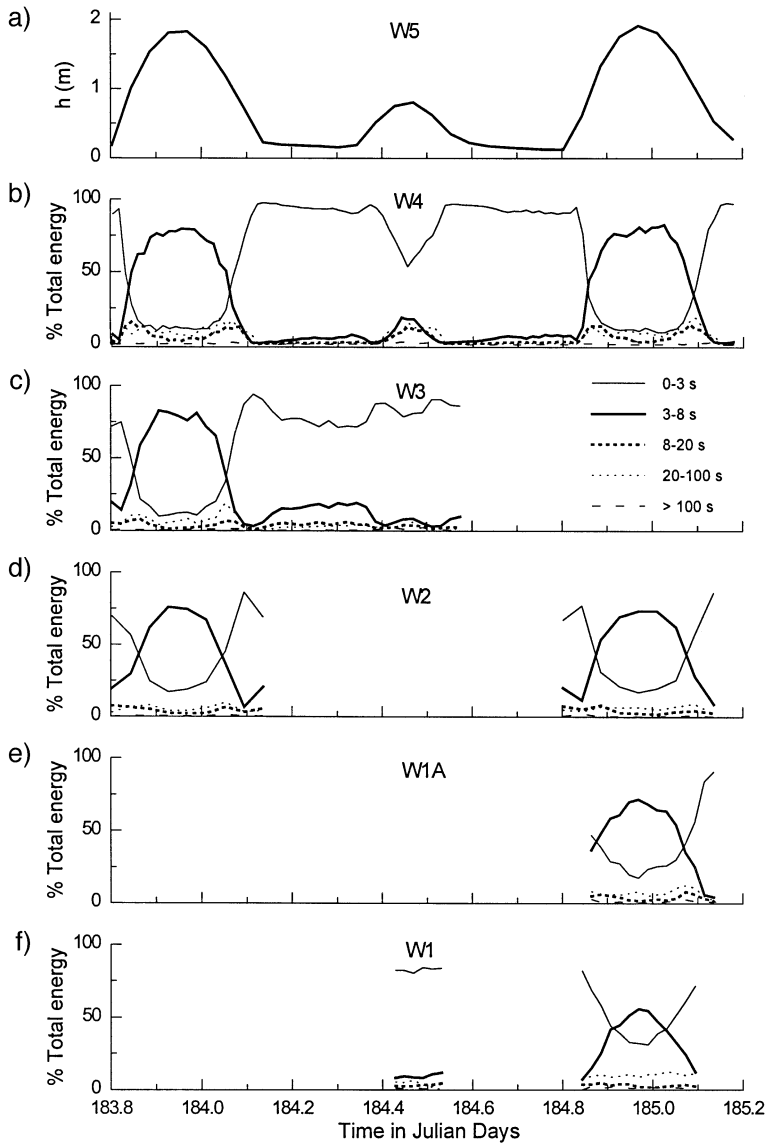

Fig. 6. Temporal variation in the percentage of total wave energy by the different wave frequency bands at each instrument location during the experiment showing: (a) water depth at W5; and energy at (b) W4; (c) W3; (d) W2; (e) W1A; and (f) W1.

the two wave types occurs at mid-tide and is characterized by distinct water level thresholds. There was a temporal progression of the occurrence of these thresholds in a landward direction across the reef. Although the reef flat is dominated by wind wave energy, this is prevalent for only a short time span (2.5 h around spring high tide), with short-period wave energy dominant for the remainder of the tidal cycle. The time of wind wave dominance also appears to diminish landward across the reef platform.

7. Discussion

Results highlight the dependence of wave processes on tidal elevation at the reef edge and across the reef

platform and indicate a number of distinct water thresholds which control wave characteristics. The spatial extent of the Warraber reef platform also exerts a major control on wave transformation and growth at different tidal stages. These results have significant geomorphological implications for sediment transport across the reef platform.

7.1. Wave attenuation

Previous studies (Roberts, 1975; Gerritsen, 1981; Roberts and Suhayda, 1983; Young, 1989; Kench, 1998; Lugo-Fernandez et al., 1998a,b) have reported a marked attenuation of incident wave energy across the reef platform ranging from 77% to 94% at low tide to 68–85% at high tide. At Warraber, mean ocean swell height (1.4 m; Young, 1999) is reduced by 65% between the reef rim and the outer reef flat (W5; Fig. 7b). At high tide, up to 85% of incident wave energy is attenuated by the central reef flat depression (W4), which is 1500 m from the shoreline. This value is similar to that reported by Lugo-Fernandez et al. (1998a,b) across a narrow 150-m bank-fringing reef in the Caribbean. Maximum wave attenuation on the Warraber reef platform is 95% (W4) and occurs just prior to reef rim exposure at lower mid-tide stages (Fig. 7b). Unlike the microtidal setting studied by Lugo-Fernandez et al. (1998a,b), the tide falls below the level of the reef crest precluding all wave energy passing over the reef crest. Also unique to this study is an increase in wave energy from the central reef flat depression to the inner reef ramp (Fig. 7a). This can likely be attributed to wave shoaling across the inner reef ramp.

7.2. Wave energy thresholds

Reef geometry and changes in water level determine the magnitude of wave energy on the reef platform. There is a general linear relationship significant at the 0.05 confidence level (R^2>0.9; Fig. 8) between H_s and h at all locations across the reef that varies spatially on the reef platform. Areas of the reef fully exposed at low tidal levels (W1, W1A) show a linear relationship (Fig. 8a, b). The linear relationship between H_s and h in the central reef locations (W2–W5) exhibits a distinct break in slope at H_s = 0.05 m. This is due to ponded water when the tide falls below

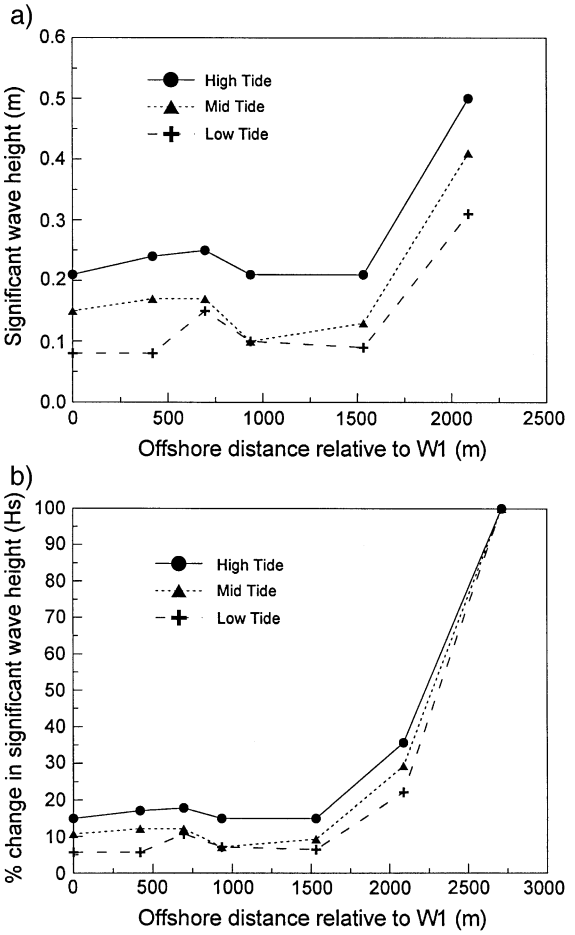

Fig. 7. Wave attenuation across the Warraber reef platform at different tidal stages showing: (a) the variation of H_s across the reef; and (b) the % change in H_s at the instrument sites relative to offshore H_s.

the level of the reef rim (Fig. 2). Any wave action at this time is solely attributed to severely fetch and depth limited waves across the ponded water surface. It is also apparent from the continuous water level records at W4 that wave heights during the rising tide are larger than the falling tide for equivalent water depths (Fig. 8e).

Gourlay (1993) reports that maximum possible wave heights on horizontal reef surfaces can be approximated by 0.55 h. Application of this relationship to the Warraber reef platform suggests that wave heights are well below this threshold and only approach it at the outer reef flat (W5; Fig. 8f). This indicates that wave energy across the reef platform is

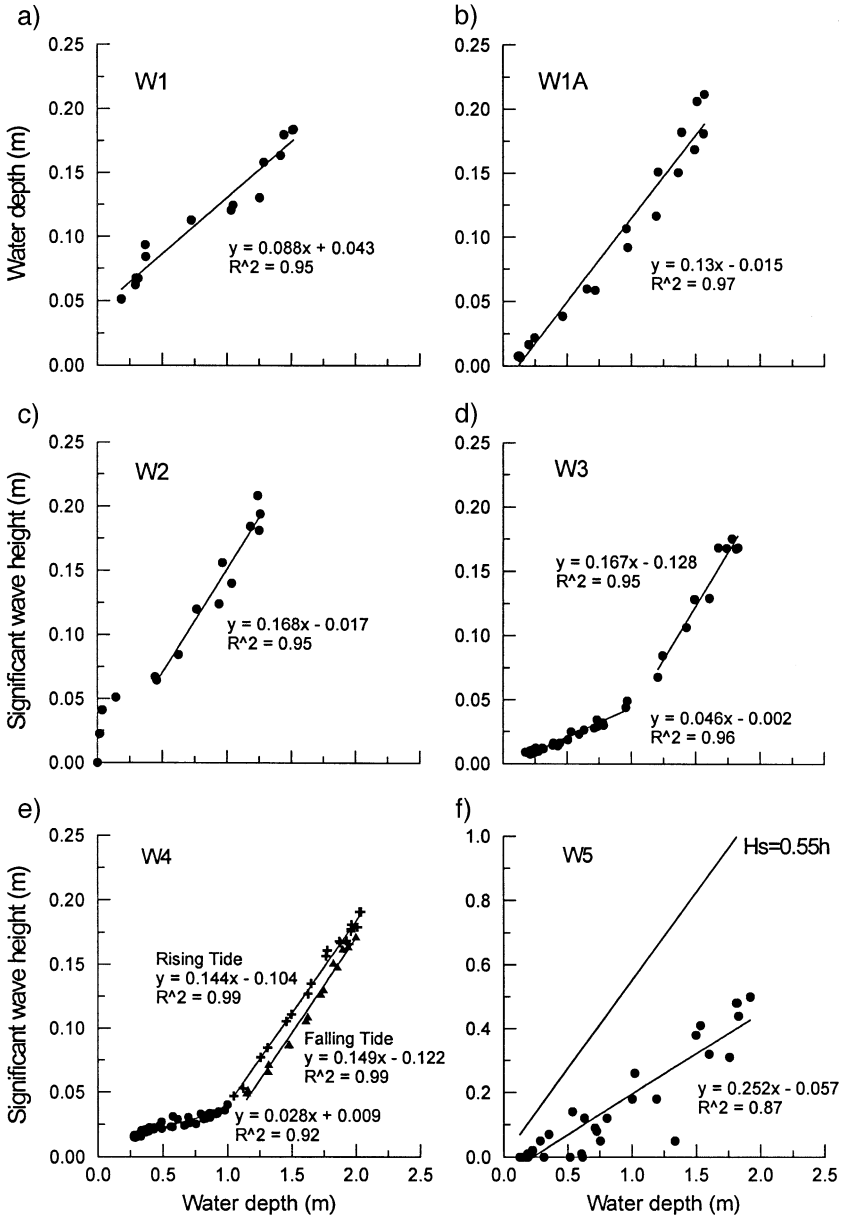

Fig. 8. Linear regression relationships between H_s and h at: (a) the shoreline (W1); (b) the palaeo reef surface (W1A); (c, d) the inner reef ramp (W2, W3); (e) central reef flat depression (W4); and (f) the outer reef flat (W5). The relationship $H_s = 0.55h$ (Gourlay, 1993) is shown in (f). All relationships are significant at the 0.05 confidence level.

unsaturated under the spring tidal conditions experienced during this study. Water level records obtained over the entire 14-day lunar tidal cycle at W5 indicate that wave heights were at a maximum during the experimental period suggesting that energy saturation on the reef would likely only occur during infrequent storm events. A physical explanation for the unsaturated character of waves on the Warraber reef platform relates to the large reef width, rapid attenuation of energy on the outer reef, and marked topographic

variations across the reef resulting in waves on the inner reef being dominated by short-period and wind waves over the fetch limited reef platform.

Numerous studies have identified critical water depths at the reef edge that allow wave energy to propagate onto the reef surface (Roberts et al., 1977; Gerritsen, 1981; Roberts and Suhayda, 1983; Kench, 1998). Fig. 9 illustrates the direct relationship between increasing significant wave height and water depth at the reef rim at each location. The critical reef rim depths required to produce H_s of a given size vary spatially across the reef platform. Critical depths increase across the central reef peaking at the inner reef ramp (W2), and water depth increments between successively higher waves are relatively constant. On the palaeo-reef and close to the shoreline, there is a relative reduction in critical reef rim water depth required to generate waves of equivalent height to those on the outer reef (Fig. 9). This is caused by the fact that the palaeo-reef is higher in elevation than the reef rim (Fig. 2). Consequently, the magnitude of water level increase to obtain greater wave heights is much larger than the central and outer reef highlighting the influence that positive relief features exert upon wave processes on reef platforms.

Results from Warraber show that water depth also controls the types of waves on the reef. Short-period waves (0–3 s) dominate the energy spectra across the reef at low water levels. At high tide, wind waves (3–8 s) dominate the wave spectra at all locations on the reef. Wave hindcast predictions using linear wave theory using the reef platform width (2.7 km), high and mid-tide water levels, and wind speed during the experiment indicate that only waves of less than $T_s = 2$ s can be locally generated across the reef platform. This suggests that wind wave energy is either generated outside the reef rim or that ocean swell wave energy experiences a shift in period associated with energy dissipation at the reef rim.

A distinct threshold exists during rising and falling water levels at which energy dominance of the short-period and wind wave frequency bands switches (Fig. 6). This threshold appears to correspond with the water depth threshold above which waves greater than 0.05 m occur at each location (Figs. 4 and 6). This threshold was shown to be depth related (Fig. 8) indicating the period of time that waves of each frequency occur at each location varies across the reef flat.

Roberts and Suhayda (1983) reported that wind waves of 5–8 s dominated the backreef environment at low tide, while longer period energy was eliminated and only propagated onto the reef at high tide. This general pattern is also observed at Warraber. However, swell wave energy (8–20 s) is minimal in the energy spectra at all locations at high tide (Fig. 5). This suggests that incident swell energy is effectively dissipated at or within a short distance across the outer reef slope and reef rim. Some of this energy may be

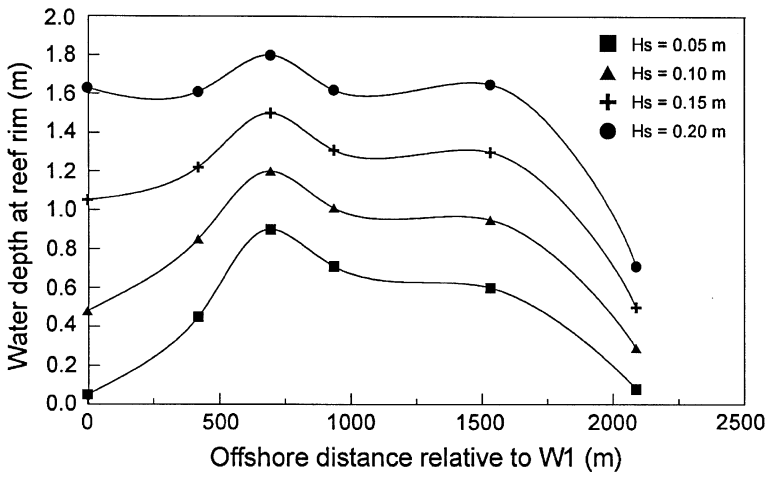

Fig. 9. Critical water depths (h) at the Warraber reef rim required to produce significant wave heights ($H_s = 0.05$, 0.10, 0.15 and 0.20 m) at each measurement location across the reef platform.

transferred to infragravity wave frequencies (>20 s) which peak at lower tidal stages at Warraber, but comprise less than 0.5% of total wave energy (Fig. 5d). These findings indicate the wave characteristics of the Warraber reef platforms are dominated by locally generated short-period waves and wind waves propagating across the reef rim at greater water depths. The rapid reduction in wave height and energy from the open sea to just landward of the reef rim (Fig. 7a) suggest the effective influence of ocean swell diminishes across the first 800 m of reef, which represents only 30% of the entire reef width. Consequently, landward of this zone waves are predominantly wind waves.

7.3. Temporal relationships

The marked water level and reef topographic controls on wave characteristics also dictates the proportion of time that waves of different height and period occur across the reef flat. Based on linear regression equations between water depth and wave height (Fig. 8), the percent occurrence of wave heights at 0.05 m increments (0.05–0.2 m) were calculated for each location over the spring tides during the experimental period (Fig. 10a). This shows that the percent occurrence of waves of specific height decreases rapidly across the outer reef flat before increasing over the inner reef ramp and palaeo reef surface. Of note, larger wave heights (e.g., $H_s = 0.2$ m), which would be expected to promote sediment entrainment and transport, decrease from 21% occurrence at the outer reef flat to <1% occurrence over the central and inner portions of the reef. Shoaling processes produce a localized increase to 4% occurrence across the inner reef ramp.

Over the 14-day spring-neap tidal cycle (as recorded at W5), the percent occurrence of these waves diminishes across the reef platform to the palaeo-reef surface (Fig. 10b). This again indicates the importance of water depth on wave height across the reef platform since at lower high tide levels, in particular, neap tides, critical water depths for geomorphically significant wave development are simply not attained. The increase of 5–10% occurrence at the shoreline of lower wave heights (Fig. 10b) reflects the importance of locally generated short-period waves and wind wave propagation across the wide reef platform at higher water levels. In contrast to the spring tide measurements (Fig. 10a), H_s of 0.2 m occur for only 9% of time at the outer reef flat (W5) and less than 0.5% over the remainder of the reef flat.

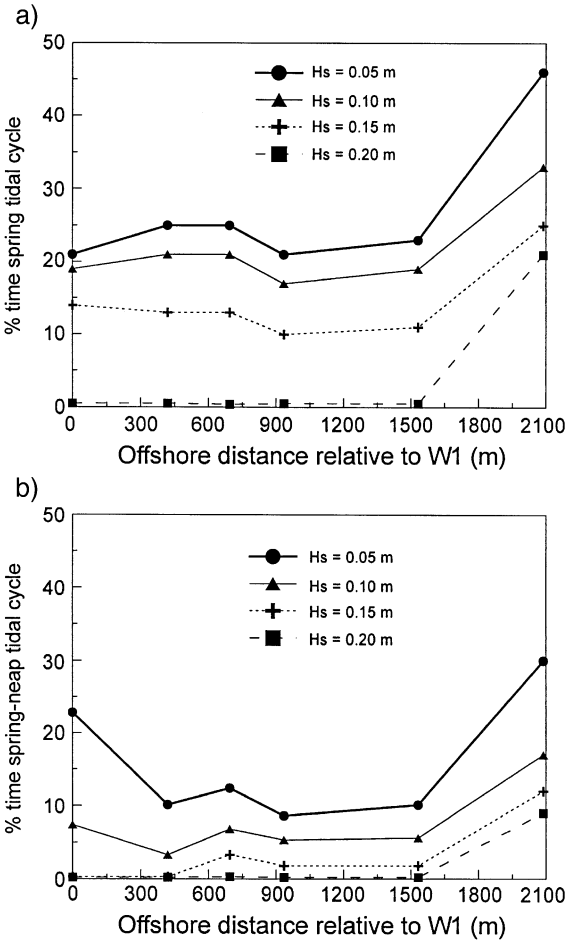

Fig. 10. Temporal representation of the time that waves of a given significant wave height ($H_s = 0.05$, 0.10, 0.15 and 0.20 m) occur across the reef platform for: (a) the spring tidal cycles measured over the experimental period; and (b) the entire 14-day spring-neap tidal cycle recorded at W5.

7.4. Geomorphological implications

These findings have several important implications towards the geomorphology of coral reef platforms and islands such as Warraber. Water level controls across the reef rim severely constrain the time that waves of sufficient energy are able to perform geomorphic work on the reef platform.

The potential for sediment entrainment across the reef platform decreases landward and transport is likely to be most active under highest water levels exhibiting bi-weekly temporal peaks associated with spring high tide conditions. Under normal energy conditions, and for the vast majority of time, the reef platform surface is geomorphologically inert. Significant changes to sediment production, transport rates and island sediment budgets are therefore likely dependant on either extreme waves or storm conditions.

8. Conclusions

The Warraber reef platform exhibits topographic variability in the form of positive relief features, a central reef flat depression, and an inner reef ramp. This variability is in marked contrast to the assumed horizontal reef surfaces of theoretical studies. Similarly, wave measurements at Warraber were made over a wide reef platform, which differs noticeably from the narrow forereef to backreef zones described by most reef hydrodynamic field studies. The results of this study have therefore added significantly to our knowledge of spatial and temporal variations in wave characteristics and energy on natural coral reef platforms. Across broad reef platforms such as Warraber, critical water depths at the reef rim have been shown to be of more importance to both the types and time of occurrence of waves acting across the reef platform than previously shown.

Previous studies have largely focussed on the role of critical water depths at the reef rim on wave attenuation and transformation across narrow reefs. The rapid decay of wave energy across the reef rim means that wave characteristics across the reef platform are more dependent on short-period and wind waves than incident swell. Furthermore, this study has shown that topographic reef platform variability does exert an influence on reef platform wave characteristics. Most importantly, however, it is clear that under normal environmental conditions, the amount of time that significant wave energy acts across the reef platform is minimal. The geomorphological implication here is that little opportunity exists for sediment transport to occur under normal energy conditions and that significant change is likely associated with extreme events. Warraber is somewhat unique in that the mesotidal ocean tide range ensures that for much of the 14-day lunar tidal cycle, water levels do not rise above the level of the reef rim. However, the findings of this study are relevant to many global reef and reef island settings. Further measurements from a range of environments and energy conditions are needed before coral reef platform and reef island morphodynamics can fully be assessed.

Acknowledgements

The authors would like to thank Roger McLean for his assistance in the field. Funding for the project was provided by a large Australian Research Council Grant awarded to Colin Woodroofe and by a UNSW URSP grant to Rob Brander. Thanks to the islanders (Ted Billy, Bogo Billy and Clara Tamu) for help and hospitality and to Douglas Jacobs of the Torres Strait Regional Authority. Prof. Ian Young of Adelaide University is thanked for providing wave climate data for the Warraber region.

References

Aagaard, T., Masselink, G., 1999. The surf zone. In: Short, A.D. (Ed.), Handbook of Beach and Shoreface Morphodynamics. Wiley, New York, pp. 72–118.

Amin, M., 1978. A statistical analysis of storm surges in Torres Strait. Aust. J. Mar. Freshw. Res. 29, 479–496.

Baird, M.E., Roughan, M.M., Brander, R.W., Middleton, J.H., Nippard, G.J., 2004. Mass transfer limited nitrate uptake on a coral reef flat, Warraber Island, Torres Strait, Australia. Coral Reefs (in press).

Bode, L., Mason, F., 1994. Tidal modelling in Torres Strait and Gulf of Papua. In: Bellwood, O., Choat, H., Saxena, N. (Eds.), Recent advances in Marine Science and Technology '94. PACON International and James Cook University, Townsville, pp. 55–65.

Fairbridge, R.W., 1950. Recent and pleistocene coral reefs of Australia. J. Geol. 58, 330–441.

Flood, P.G., 1974. Sand movements on Heron Island—a vegetated sand cay, Great Barrier Reef province, Australia. Proc. 2nd Int. Coral Reef Symposium, Great Barrier Reef Committee, Brisbane, pp. 387–394.

Frith, C.A., 1982. Circulation in a platform reef lagoon, One Tree Reef, southern Great Barrier Reef. Proc. 4th Int. Coral Reef Symposium. ASCE, Quezon City, pp. 347–354.

Frith, C.A., Mason, L.B., 1986. Modelling wind-driven circulation, One Tree Reef, southern Great Barrier Reef. Coral Reefs 4, 201–211.

Gerritsen, F., 1981. Wave attenuation and wave set-up on a coastal reef. Proc. 17th Int. Conf. Coast. Eng. ASCE, Sydney, pp. 444–461.

Gourlay, M.R., 1988. 'Coral Cays' products of wave action and geological processes in a biogenic environment. Proc. 6th Int. Coral Reef Symposium, Great Barrier Reef Committee, Townsville, Australia, pp. 491–496.

Gourlay, M.R., 1990. Wave setup and currents on reefs-cay formation and stability. Proc. Eng. Coral Reef Regions Conf., 163–178.

Gourlay, M.R., 1993. Wave setup and wave generated currents on coral reefs. Proc.11th Aust. Conf. Coastal and Ocean Eng. IEA, Townsville, pp. 479–484.

Gourlay, M.R., 1994. Wave transformation on a coral reef. Coast. Eng. 23, 17–42.

Gourlay, M.R., 1996a. Wave set-up on coral reefs: 1. Set-up and wave generated flow on an idealised two dimensional horizontal reef. Coast. Eng. 27, 161–1935.

Gourlay, M.R., 1996b. Wave set-up on coral reefs: 1. Set-up on reefs with various profiles. Coast. Eng. 28, 17–55.

Hardy, T.A., Young, I.R., 1991. Modeling spectral wave transformation on a coral reef flat. Proc. 10th Aust. Conf. Coastal and Ocean Eng. Austr. Inst. of Eng., Auckland.

Hardy, T.A., Young, I.R., Nelson, R.C., Gourlay, M.R., 1991. Wave attenuation on an offshore coral reef. Proc. 22nd Int. Conf. Coast. Eng. ASCE, Delft, pp. 330–344.

Harris, P.T., 1988. Sediments, bedforms and bedload transport pathways on the continental shelf adjacent to Torres Strait, Australia–Papua New Guinea. Cont. Shelf Res. 8 (8), 979–1003.

Hearn, C.J., 1999. Wave-breaking hydrodynamics within coral reef systems and the effect of changing relative sea level. J. Geophys. Res. 104 (C12), 30007–30019.

Hearn, C.J., Parker, I.N., 1988. Hydrodynamic processes on the Ningaloo coral reef, Western Australia. Proc. 6th Int. Coral Reef Symp., Great Barrier Reef Comm., Townsville, pp. 497–502.

Hearn, C.J., Atkinson, M.J., Falter, J.L., 2001. A physical derivation of nutrient-uptake rates in coral reefs: effects of roughness and waves. Coral Reefs 20, 347–356.

Hopley, D., 1981. Sediment movement around a coral cay, Great Barrier Reef, Australia. Pac. Geol. 15, 17–36.

Hopley, D., 1982. The Geomorphology of the Great Barrier Reef: Quaternary Development of Coral Reefs. Wiley, New York.

Jennings, J.N., 1972. Some attributes of Torres Strait. In: Walker, D. (Ed.), Bridge and Barrier: the Natural and Cultural History of Torres Strait. A.N.U. Res. Sch. Pacific Stud. Publ., vol. BG/3, ANU Press, Canberra, pp. 29–38.

Kench, P.S., 1994. Hydrodynamic observations of the Cocos (Keeling) Islands lagoon. Atoll Res. Bull. 408, 21.

Kench, P.S., 1998. Physical processes in a semi-enclosed Indian Ocean atoll. Coral Reefs 17, 155–168.

Kraines, S.B., Yanagi, T., Isobe, M., Komiyama, H., 1998. Wind-wave driven circulation on the coral reef at Bora Bay, Miyako Island. Coral Reefs 17, 133–143.

Lee, T.T., Black, K.P., 1987. The energy spectra of surf waves on a coral reef. Proc. 16th Int. Conf. Coast. Eng. ASCE, Hamburg, pp. 588–608.

Lugo-Fernandez, A., Roberts, H.H., Wiseman Jr., W.J., 1998a. Tide effects on wave attenuation and wave set-up on a Caribbean Coral Reef. Estuar. Coast. Shelf Sci. 47, 385–393.

Lugo-Fernandez, A., Roberts, H.H., Wiseman, W.J., Carter, B.L., 1998b. Water level and currents of tidal and infragravity periods at Tague Reef, St Croix (USVI). Coral Reefs 17, 343–349.

Massel, S.R., 1992. Wave transformation and dissipation on steep reef slopes. Proc. 11th Aust. Fluid Mechanics Conf., Hobart, Tasmania, pp. 319–322.

McLean, R.F., Stoddart, D.R., 1978. Reef island sediments of the northern Great Barrier Reef. Philos. Trans. R. Soc. Lond., A 291, 101–117.

Nelson, R.C., 1996. Hydraulic roughness of coral reef platforms. Appl. Ocean Res. 18, 265–274.

Prager, E.J., 1991. Numerical simulation of circulation in a Caribbean-type backreef lagoon. Coral Reefs 10, 177–182.

Roberts, H.H., 1975. Physical processes in a fringing reef system. J. Mar. Res. 33, 233–260.

Roberts, H.H., Suhayda, M., 1983. Wave current interactions on a shallow reef (Nicaragua). Coral Reefs 1, 209–260.

Roberts, H.H., Murray, S.P., Suyhayda, J.N., 1977. Physical processes in a fore-reef shelf environment. Proc. 3rd Int. Coral Reef Symposium, ASCE, Miami, pp. 507–515.

Roberts, H.H., Wilson, P.A., Lugo-Fernandez, A., 1992. Biologic and geologic responses to physical processes: examples from modern reef systems of the Caribbean–Atlantic region. Cont. Shelf Res. 12 (7/8), 809–834.

Seelig, W., 1983. Laboratory study of reef–lagoon system hydraulics. J. Waterw. Port Coast. Ocean Eng. 109, 380–391.

Spender, M.A., 1930. Island reefs of the Queensland coast. Geog. J., 76, 194–214, 273–297.

Steers, J.A., 1937. The coral islands and associated features of the Great Barrier Reefs. Geog. J., 89, 1–28, 119–146.

Stoddart, D.R., Steers, J.A., 1977. The nature and origin of coral reef islands. In: Jones, O.A., Endean, R. (Eds.), Biology and Geology of Coral Reefs, vol. 4. Academic Press, New York, pp. 59–105.

Symonds, G., 1994. Theory and observation of currents and setup over a shallow reef. Proc. Coastal Dynamics '94. ASCE, Barcelona, pp. 1–13.

Symonds, G., Black, K.P., Young, I.R., 1995. Wave-driven flow over shallow reefs. J. Geophys. Res. 100 (C2), 2639–2648.

Tait, R.J., 1972. Wave setup on coral reefs. J. Geophys. Res. 77, 2207–2211.

Tartinville, B., Rancher, J., 2000. Wave-induced flow over Mururoa Atoll reef. J. Coast. Res. 16 (3), 776–781.

Tsukayama, S., Nakaza, E., 2001. Wave transformations on coral reefs. Proc. 27th Int. Conf. Coast. Eng. ASCE, Sydney, pp. 1372–1382.

Wolanski, E., King, B., 1990. Flushing of Bowden Reef lagoon, Great Barrier Reef. Estuar. Coast. Shelf Sci. 31, 789–804.

Woodroffe, C.D., Kennedy, D.M., Hopley, D., Rasmussen, C.E., Smithers, S.G., 2000. Holocene reef growth in Torres Strait. Mar. Geol. 170, 331–346.

Yamano, H., Kayanne, H., Yonekura, N., Nakamura, H., Kudo, K., 1998. Water circulation in a fringing reef located in a monsoon area: Kabira Reef, Ishigaki Island, Southwest Japan. Coral Reefs 17, 89–99.

Young, I.R., 1989. Wave transformation over coral reefs. J. Geophys. Res. 94, 9779–9789.

Young, I.R., 1999. Seasonal variability of the global ocean wind and wave climate. Int. J. Climatol. 19, 931–950.